




Atypical development of Broca's area in a large family with inherited stuttering

 Daisy G. Y. Thompson-Lake,¹ Thomas S. Scerri,^{2,3} Susan Block,⁴ Samantha J. Turner,⁵ Sheena Reilly,^{5,6} Elaina Kefalianos,^{5,7} Alexandra F. Bonthron,¹ Ingo Helbig,^{8,9,10,11}  Melanie Bahlo,^{2,3} Ingrid E. Scheffer,^{12,13,14,15} Michael S. Hildebrand,^{12,14} Frédérique J Liégeois^{1,†} and  Angela T. Morgan^{5,7,13,†}

[†]These authors contributed equally to this work.

Developmental stuttering is a condition of speech dysfluency, characterized by pauses, blocks, prolongations and sound or syllable repetitions. It affects around 1% of the population, with potential detrimental effects on mental health and long-term employment. Accumulating evidence points to a genetic aetiology, yet gene–brain associations remain poorly understood due to a lack of MRI studies in affected families. Here we report the first neuroimaging study of developmental stuttering in a family with autosomal dominant inheritance of persistent stuttering.

We studied a four-generation family, 16 family members were included in genotyping analysis. T₁-weighted and diffusion-weighted MRI scans were conducted on seven family members (six male; aged 9–63 years) with two age and sex matched controls without stuttering ($n = 14$). Using Freesurfer, we analysed cortical morphology (cortical thickness, surface area and local gyrification index) and basal ganglia volumes. White matter integrity in key speech and language tracts (i.e. frontal aslant tract and arcuate fasciculus) was also analysed using MRtrix and probabilistic tractography.

We identified a significant age by group interaction effect for cortical thickness in the left hemisphere pars opercularis (Broca's area). In affected family members this region failed to follow the typical trajectory of age-related thinning observed in controls. Surface area analysis revealed the middle frontal gyrus region was reduced bilaterally in the family (all cortical morphometry significance levels set at a vertex-wise threshold of $P < 0.01$, corrected for multiple comparisons). Both the left and right globus pallidus were larger in the family than in the control group (left $P = 0.017$; right $P = 0.037$), and a larger right globus pallidus was associated with more severe stuttering ($\rho = 0.86$, $P = 0.01$). No white matter differences were identified. Genotyping identified novel loci on chromosomes 1 and 4 that map with the stuttering phenotype.

Our findings denote disruption within the cortico-basal ganglia-thalamo-cortical network. The lack of typical development of these structures reflects the anatomical basis of the abnormal inhibitory control network between Broca's area and the striatum underpinning stuttering in these individuals. This is the first evidence of a neural phenotype in a family with an autosomal dominantly inherited stuttering.

- 1 UCL Great Ormond Street Institute of Child Health, London, UK
- 2 Population Health and Immunity Division, The Walter and Eliza Hall Institute of Medical Research, 1G Royal Parade, Parkville 3052, Australia
- 3 Department of Medical Biology, University of Melbourne, 1G Royal Parade, Parkville 305, Australia
- 4 Discipline of Speech Pathology, School of Allied Health, Human Services & Sport, La Trobe University, Bundoora 3086, Australia
- 5 Speech and Language, Murdoch Children's Research Institute, Parkville 3052, Australia

Received April 20, 2021. Revised August 9, 2021. Accepted August 24, 2021. Advance access publication November 23, 2021

© The Author(s) (2021). Published by Oxford University Press on behalf of the Guarantors of Brain. All rights reserved. For permissions, please email: journals.permissions@oup.com

- 6 Menzies Health Institute Queensland, Griffith University, Southport 4215, Australia
- 7 Department of Audiology and Speech Pathology, University of Melbourne, Parkville 3052, Australia
- 8 Division of Neurology, Children's Hospital of Philadelphia, Philadelphia, PA 19104 USA
- 9 The Epilepsy NeuroGenetics Initiative, Children's Hospital of Philadelphia, Philadelphia, PA 19104 USA
- 10 Department of Biomedical and Health Informatics, Children's Hospital of Philadelphia, Philadelphia, PA 19104 USA
- 11 Department of Neurology, University of Pennsylvania, Perelman School of Medicine, Philadelphia, PA 19104 USA
- 12 Department of Medicine, University of Melbourne, Austin Hospital, Heidelberg 3084, Australia
- 13 Department of Paediatrics, University of Melbourne, Royal Children's Hospital, Parkville 3052, Australia
- 14 Murdoch Children's Research Institute, Parkville 3052, Australia
- 15 Florey Institute of Neuroscience and Mental Health, Parkville 3052, Australia

Correspondence to: Angela T. Morgan
 Murdoch Children's Research Institute
 Parkville 3052, Australia
 E-mail: angela.morgan@mcri.edu.au

Keywords: cortical thickness; inherited stuttering; Freesurfer; Broca's area; basal ganglia

Abbreviations: CST = corticospinal tract; DWI = diffusion-weighted imaging; FAT = frontal aslant tract; GLM = general linear model; IFG = inferior frontal gyrus

Introduction

Developmental stuttering is a condition of speech dysfluency, characterized by blocks, prolongations and repetitions. Stuttering onset is most commonly between 2 and 4 years of age,¹ with 65% of children recovering by 7 years.² In adulthood, stuttering remains highly prevalent, affecting around 1% of the population.³ It is associated with negative impacts on psychological well-being, educational opportunities,⁴ career progression and earnings.⁵ Additionally, interpersonal relationships and overall quality of life may be greatly affected.^{6,7} Individuals who stutter experience a 2-fold increase in psychiatric disorders, including anxiety, depression and suicidal ideation, compared to the general population.⁸

While the genetic architecture for stuttering is poorly understood, evidence from twin and adoption studies^{9,10} suggests a significant genetic contribution. Heritability estimates are often >0.8, and concordance for stuttering is higher in monozygotic compared to dizygotic twins.^{9,10} Monogenic contributions of relevance to the general population with stuttering remain elusive despite decades of investigation. Rare variants of lysosomal targeting pathway genes (GNPTAB, GNPTG and NAGPA) were initially identified in consanguineous Pakistani families with non-syndromic persistent stuttering, and later in unrelated Pakistani and North American cases.¹¹ Recent evidence has linked these genes to both grey matter volumetric differences in stuttering¹² and to functional connectivity within the stuttering network.¹³ Rare loss of function variants in AP4E1 have also been described in individuals with stuttering from Cameroon and Pakistan. AP4E1 encodes a protein that is functionally related to the lysosomal targeting pathway.^{9,14} Distinct genetic variants may target different neuronal pathways or brain structures, and yet, still culminate in the same behavioural phenotype of stuttering. This phenomenon is seen in other speech disorders such as childhood apraxia of speech, where reductions of the caudate nucleus have been replicated in individuals with FOXP2 variants^{15,16} but not observed in other cases without known genetic determinants.¹⁷ Thus, in speech disorders, genetic heterogeneity may underpin inconsistent neuroimaging findings. Despite extensive neuroimaging research in stuttering over the last few decades, investigation of

neural phenotypes in genetically homogenous individuals is notably absent.

Structural neuroimaging studies of individuals who stutter have identified differences in both the volumes of, and connections between, regions of the cortex concerned with speech motor control.^{18–21} In both children and adults, there has been converging evidence of reduced integrity of white matter underlying the left rolandic cortex²² and in the arcuate fasciculus.^{23–28} This dorsal language pathway²⁹ connects the posterior superior temporal gyrus, auditory processing regions, to the left inferior frontal gyrus (IFG, Broca's area). Various white matter pathways have been implicated outside these speech-related tracts. Recent evidence indicates reduced integrity of the frontal aslant tract (FAT) which connects the IFG with the presupplementary motor area, supplementary motor area and anterior cingulate cortex.^{30,31} Although adults who stutter demonstrate increased mean diffusivity in the left FAT and preserved fractional anisotropy,³² children present with increased fractional anisotropy in the right FAT³³. Overall, there is strong evidence of white matter alterations in individuals who stutter, but the location and characteristics of these perturbations vary.

In addition to white matter, grey matter anomalies have been identified in both the basal ganglia-thalamo-cortical and auditory-motor networks in the left hemisphere.^{25,34} Both increased and decreased grey matter volume within the same cortical regions have been reported.^{18,21,35,36} Yet there is extensive evidence of reduced grey matter in the left IFG (Broca's area) and ventral premotor cortex in both children and adults^{21,36–39} and of increased grey matter volume in the right precentral and superior temporal gyrus.^{34,40,41} Investigations of subcortical structures in adults have demonstrated increased volume of the left putamen,³⁴ as well as reductions in the left caudate nucleus.⁴² In contrast, studies in children have found volumetric increases in the right caudate,⁴³ and reductions in the left putamen.³⁷ Thus, it is critical to acknowledge that brain anomalies associated with stuttering may change with age and may vary depending on the underlying genetic contributions to symptomatology.

Here we establish the neural phenotype associated with a strong history of inherited stuttering in this four-generation family. Structural and diffusion MRI enabled measures of cortical

morphometry, subcortical volumes and white matter integrity in the arcuate fasciculus, frontal aslant, corticobulbar (CBT) and corticospinal (CST) tracts. We also examined the relationship between stuttering severity and subcortical volumes. In parallel, we used linkage analysis to map genetic loci since the inheritance pattern in the family appeared consistent with transmission of a single, rare autosomal dominant allele of large effect causing a monogenic form of stuttering. To identify gene variants of interest at the genetic loci, we then performed exome sequencing.

Materials and methods

Family

We studied a four-generation Australian family of Caucasian origin segregating persistent developmental stuttering (Fig. 1 and Table 1). All family members over the age of 5 years were invited to take part in an MRI scan, and seven agreed to take part: 16 family members were genotyped (Fig. 1). None of the family members had any diagnosis of psychiatric, neurodevelopmental or neurological disorder, as ascertained via an extensive health and medical interview in person including a follow-up written survey, as well as confirming this via accessing family health records. The Human Research Ethics Committee of the Royal Children's Hospital, Melbourne, Australia (HREC 37353), approved the study. Written informed consent was obtained according to the Declaration of Helsinki from participants, or their parents or legal guardians in the case of minors.

Speech and cognitive phenotypes

Qualified speech pathologists (A.M., S.B., S.T.) assessed family members (see Table 1 for individual profiles). Stuttering severity was confirmed by a case history, observation of stuttering behaviours and calculating percent syllables stuttered (%SS), with $\geq 2\%$ SS denoting a clinical diagnosis. Ratings were based on 5 minutes of audio-recorded conversational speech and averaged across three raters who were qualified speech pathologists experienced in stuttering assessment (S.B., E.K., S.T.). Raters provided a description of all stuttering behaviours (Table 2) observed during each of the speech samples. Participants also provided a self-report of stuttering status, indicating whether they identified as a person with persistent or recovered stuttering. Verbal and non-verbal IQ were measured using standardized tests⁴⁴ (Table 1).

All participants were monolingual English speakers, each family member was matched to two control participants based on age, sex, handedness, ethnicity, education and socio-economic status. Control participants had no history of speech or language disorder, medical or neurodevelopmental conditions and no contraindications for MRI scanning.

Biological samples

Whole blood or saliva was obtained from family members. For blood, genomic DNA was extracted using the Qiagen QIAamp DNA Maxi Kit. For saliva obtained using the Oragene kit, genomic DNA was extracted using the prepIT L2P kit (DNA Genotek Inc.).

SNP genotyping and linkage analysis

Sixteen family members (I-1, I-2, II-1, II-2, II-3, II-5, II-6, III-1, III-2, III-4, III-9, III-12, III-13, IV-1, IV-2 and IV-3; Fig. 1) were genotyped on Illumina OMNI Express Arrays with genotyping call rates above 99.5% for all samples. Genotyping data were pre-processed for genotype calls, sex and Mendelian errors using Linkdatagen⁴⁵ before parametric and non-parametric multipoint linkage analysis using MERLIN⁴⁶. Parametric linkage analysis was performed specifying a rare dominant allele population frequency of 0.001, a penetrance of 0.0001 for homozygous wild-type individuals and a penetrance of 1.000 for heterozygous or homozygous carriers of the disease allele. Haplotypes were determined through visual inspection of plots produced by HaploPainter.⁴⁷

Brain MRI acquisition and processing

Eighteen participants underwent MRI imaging acquired with a 3.0T Siemens Trio Tim scanner at the Brain Research Institute in Melbourne, Australia. One hundred and sixty T₁-weighted images were obtained using an MP-RAGE sequence (TR = 1900 ms, TE = 2.5 ms, flip angle of 9°, voxel size = 1 × 1 × 1 mm³). Due to a contraindication with participant weight, one of the family members and their two age-matched controls were scanned on a Siemens SKYRA scanner (III-1) (number of slices = 160, TR = 1900 ms, TE = 2.6 ms, flip angle = 9°, voxel size = 1 × 1 × 1 mm³).

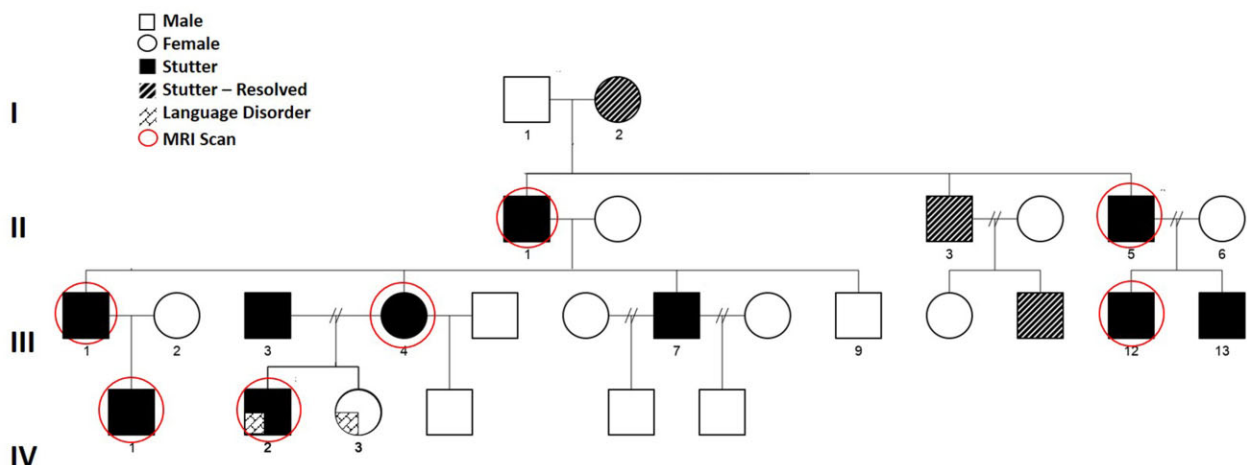


Figure 1 Australian family with persistent developmental stuttering. Sixteen family members (indicated by numbers) from the four-generation family were genotyped, and seven of those were scanned (circled in red). Circles represent females and squares represent males.

Table 1 Clinical features of scanned family members

Pedigree	Age at behavioural testing (years; months) ^a	Sex	Percentage syllables stuttered (%)	Self-report stuttering status	Verbal IQ (vocabulary)	Non-verbal IQ (matrix reasoning)	Summary IQ (verbal + non-verbal)	Language scores (PPVT-4- adults CELF-4-children)	Radiologist notes (Supplementary Fig. 2)
II-1	58; 7	Male	1.9	Persistent	10	12	107	99	Unusual sulcation left anterior cingulate—interrupted sulcus with straightened morphology and generalized atrophy that is particularly prominent in the parietal regions. Left cingulate gyrus—abnormal morphology, straight regions, interrupted and branching anterior cingulate. Unusual sulcus extending anteriorly through left superior frontal gyrus from left precentral. Normal variant.
II-5	53; 1	Male	5.8	Persistent	5	11	88	90	Marked enlargement of the extra-axial CSF spaces overlying the central and parietal regions bilaterally. Medial lesion [7 × 7 × 11 mm (TV × AP × CC)] involving anterior ramus of cingulate sulcus/rostral medial frontal cortex with blurring of grey matter and signal change in adjacent subcortical white matter.
III-1 ^b	35; 5	Male	1.8	Persistent	8	12	99	101	Large CSF space in the posterior fossa behind the cerebellar vermis in keeping with a mega cisterna magna.
III-4	31; 11	Female	2.6	Persistent	7	12	97	95	Origin of the left precentral sulcus as a branch of the left central sulcus and abnormal ramus extending laterally in the superior frontal gyrus; abnormal course of the left precentral sulcus that crosses the superior frontal gyrus to the midline.
III-12	26; 9	Male	4.2	Persistent	9	15	114	88	Abnormal left lateral temporal sulcation- ramus crossing superior temporal gyrus to join sylvian fissure; elongation of back of sylvian fissure; radiating sulci.
IV-1	7; 11	Male	7.3	Persistent	11	13	118	86	Asymmetrical hippocampi—smaller left hemisphere. Right anterior temporal arachnoid cyst causing mass effect on the right anterior temporal lobe which is displaced posteriorly and laterally. The anterior temporal pole is hypoplastic/dysplastic.
IV-2	12; 9	Male	10.2	Persistent	3	6	73	68	

^aDue to the size of the family and the geographical locations of individual members within Australia, behavioural testing and MRI data could not be collected within the same month. As a result, age at scan and at behavioural testing differs.

^bScanned on SKYRA.

Table 2 Features of stuttering phenotype of scanned family members

Pedigree	Sound repetition	Part word repetition	Whole word repetition	Phrase repetition	Blocks	Sound prolongations	Interjections	Avoidance (word)
II-1	X		X	X	X	X	X	X
II-5	X	X	X	X	X		X	X
III-1	X		X	X	X	X	X	
III-4	X		X	X	X	X	X	X
III-12	X		X	X	X	X	X	X
IV-1	X		X	X	X		X	
IV-2	X		X		X	X	X	

X = feature is present.

Diffusion-weighted images

The diffusion-weighted imaging (DWI) data were acquired for 9 min with the following sequence parameters: field of view 240 × 240 mm; 60 contiguous axial slices, a 96 × 96 matrix; TR/TE = 8300/110 ms; voxel size: 2.5 × 2.5 × 2.5 mm³; b-value of 3000 s/mm². On the SKYRA, TR/TE was 8800/110 ms, with 68 volumes (64 directions).

Cortical morphometry reconstruction

Data were processed using the Freesurfer v.6.0.0 recon-all pipeline in order to produce 3D images and surface reconstructions from T₁-weighted images.^{48–50} All images were processed using a Mac OS X10.7. Details of the pipeline can be found online (<https://surfer.nmr.mgh.harvard.edu/>; accessed 8 February 2022). In brief, this involves intensity correction, skull stripping and noise filtering, identification of white matter, separation of the hemispheres and creation of a tessellated mesh representation of the white matter boundary and the pial surface.

Data were mapped to the *fsaverage* template and smoothed with a full width half maximum kernel of 10 mm. Cortical regions were parcellated into 34 regions per hemisphere according to the Desikan–Killiany atlas. Due to radiological abnormalities in the family, all data were manually inspected for accuracy of registration to the template by examining overlays of the cortical and subcortical parcellations onto each anatomical image, slice by slice along each axis. The non-linear registration used in the Freesurfer pipeline resulted in the registration being unaffected by the macroanomalies. Where necessary, we manually edited the pial surface or white matter regions that were incorrectly identified by the Freesurfer automatic registration. These edits were made for both controls and family members according to the Freesurfer guidelines (<https://surfer.nmr.mgh.harvard.edu/fswiki/FsTutorial/TroubleshootingDataV6.0>; accessed 8 February 2022), and none were in the location of macroanomalies. Cortical and subcortical parcellations were re-examined on any edited output to ensure successful registration.

Diffusion-weighted imaging analysis

Images were visually inspected for signal dropout caused by motion during acquisition of the sequence. All diffusion-weighted images were analysed using a standard pipeline in MRtrix3 software package⁵¹ (www.mrtrix.org; accessed 8 February 2022) and underwent the following procedures: (i) thermal noise correction to improve signal to noise ratio⁵²; (ii) correction for susceptibility induced distortions using TOPUP in FSL^{53–55}; (iii) motion correction using an outlier replacement strategy and eddy current correction using EDDY in FSL⁵⁴; and (iv) correction for bias field inhomogeneity using ANTS N4 tools⁵⁶; and (v) global intensity normalization.

One family member (III-I), and their two corresponding controls were scanned on the SKYRA did not have a DWI dataset with the same imaging parameters and were therefore removed from the diffusion analysis. Another family member (IV-I) had excessive movement during the scan and was excluded along with his controls. There were five family members (II-I, II-5, III-4, III-12, IV-2) and 10 controls in the final DWI analysis.

Tractography

Probabilistic tractography using constrained spherical deconvolution⁵⁷ was conducted to create fibre orientation distributions. CST and CBT tractography was conducted according to previously published methods.^{16,17,58} Tractography of the anterior segment of the arcuate fasciculus (AF) was performed according to the methods from Liegeois et al.⁵⁸ Tractography of the FAT was carried out using parcellations of the supplementary motor area and pars opercularis. NiftyReg^{59–62} was used to extract parcellations by registering the T₁-weighted image to the DWI scan and non-linearly registering the automated anatomical labelling template⁶³ (<https://www.gin.cnrs.fr/en/tools/aal/>; accessed 8 February 2022) to each participant's T₁-weighted scan in DWI space. Four binary masks of the left and right supplementary motor area and pars opercularis were extracted. Parcellations were overlain onto the DWI images and manually edited to exclude fibres from the CST and AF. The maximum number of streamlines generated was set at 100 000 and a maximum of 1000 streamlines were retained.

Data analysis

Cortical morphometry

Using a surfaced-based whole brain approach, cortical thickness, cortical surface area and local gyrification were compared between the family and controls, with age as a covariate, using a vertex-wise general linear model (GLM) in Freesurfer's Query, Design, Estimate, Contrast module. Corrections for multiple comparisons were implemented using a Monte Carlo simulation (10 000 iterations) with a cluster-wise threshold of $P < 0.05$. For *post hoc* analyses of the regions within the significant cluster (**Supplementary material**) we extracted values from the regions within the significant clusters resulting from this GLM analysis and conducted univariate analyses in IBM SPSS v.24 to determine the significance level and effect size of each region within the cluster.

All remaining additional analyses were conducted in SPSS v.24. Global grey matter, white matter, cerebrospinal fluid and total intracranial volume were compared using a non-parametric Mann–Whitney U-test with values extracted from Freesurfer's 'aseg' output. Hemisphere cortical thickness was analysed using mean thickness provided from Freesurfer's 'aparc' output. Left and right hemisphere mean thickness was entered into a multivariate

analysis of covariance (ANCOVA), with group as a main factor and age as a covariate.

Subcortical region analyses

The volumes of the basal ganglia (caudate, putamen and pallidum) were extracted as a percentage of total estimated intracranial volume. Left and right hemisphere volumes were combined for each structure due to their high collinearity. To account for modest sample sizes, we conducted Bayesian statistical analysis in support of the null hypothesis (i.e. no differences between the family and controls) using JASP Team.⁶⁴ Bayes factors were calculated using the default Cauchy's prior width (0.07) and a Monte Carlo simulation of 5000 iterations. For structures where evidence supported differences between the two groups, we conducted Mann-Whitney U-tests. Finally, for structures where a group difference was identified, we examined the relationship between volumes and stuttering severity in family members using a bivariate Spearman's rank correlation. Bayes factors were determined with a Bayesian Pearson's correlation. As there was no significant correlation between age and stuttering severity ($\rho = -0.68$; $P = 0.09$), age was not used as a covariate.

Diffusion-weighted imaging analysis

Volumes, mean fractional anisotropy and mean diffusivity were extracted for all tracts. Tract metrics from each hemisphere were entered into two separate MANOVA models with group (family versus controls) as a main factor and age as a covariate. We further compared DWI metrics with a Bayesian Mann-Whitney U-test using the default Cauchy prior width, as in Liegeois et al.¹⁷

Data availability

The data that support the findings of this study are available from the corresponding author on reasonable request.

Results

Neuroimaging was performed on seven affected family members (aged 9–63 years) and an age and gender matched control group

($n = 14$) ($P > 0.97$). The mean full scale IQ score of the family fell within the average range [mean (standard deviation, SD): 98.1(13.0), range 73–114; see Table 1 for individual IQ and language scores] and did not differ from that of controls [108 (11.2), range 92–130; $t(19) = -1.7$, $P > 0.09$]. There were no differences between groups in either verbal or non-verbal IQ subscales ($P > 0.76$). All family members self-identified as having persistent stuttering (Table 1). Stuttering severity ratings by speech pathologists ranged from mild to moderate, with an average of 4.8% syllables stuttered (SD = 3.15, range 1.8–10.2; Table 2 for individual stuttering features).

Radiological brain abnormalities in the family

We noted macrostructural anomalies on the T₁-weighted images of all family members. These findings varied in size or location and were not considered clinically relevant (Fig. 2 for examples and Supplementary Fig. 2 for individual findings) after review by an experienced neuroradiologist. Additional analyses accounting for any anomalies that may encroach on significant regions can be found in the Supplementary material.

Global brain volumes

There were no significant differences between groups in either global grey matter volume (family median = 708.79 cm³; control median = 744.65 cm³; $U = 40.0$, $P = 0.50$); white matter volume (family median = 412.67 cm³; control median = 484.75 cm³; $U = 28.0$, $P = 0.12$); total ventricular CSF (family median = 25.68 cm³; control median = 22.82 cm³; $U = 34.0$, $P = 0.26$) or estimated total intracranial volume (family median = 1515.65 cm³; control median = 1545.95 cm³; $U = 41.0$, $P = 0.55$).

Cortical thickness in Broca's area decreases with age in the control group but not in affected family members

A vertex-wise GLM analysis of thickness confirmed there was no significant group difference in any cortical region with age as covariate. There was, however, a significant age by group interaction effect in the left hemisphere pars opercularis (cluster size:

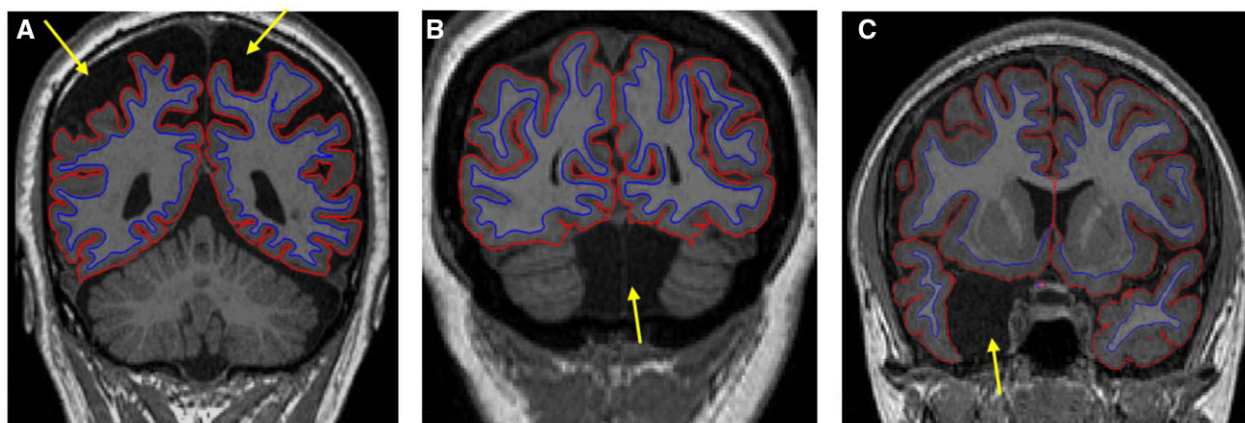


Figure 2 Examples of macroscopic brain MRI anomalies in family members. (A) Marked enlargement of extra-axial CSF disproportionate to age-related atrophy. Unknown if cause is malformative or atrophic in origin (seen in $n = 2$ family members). (B) Mega cisterna magna with increased retrovermian CSF ($n = 1$). (C) Right hemisphere middle cranial fossa arachnoid cyst with mass effect on right anterior temporal pole ($n = 1$). Other anomalies (not shown) in family members include: (i) abnormal morphology of left cingulate ($n = 3$) including interrupted anterior cingulate, straightened morphology and branching of anterior cingulate; (ii) round lesion in branch of left anterior cingulate sulcus ($n = 1$); (iii) atypical sulcation in left hemisphere ($n = 2$), including extending of left superior frontal gyrus from precentral gyrus, ramus crossing superior temporal gyrus to join sylvian fissure; elongation of back of sylvian fissure and radiating sulci; and (iv) asymmetrical hippocampi ($n = 1$) smaller left hippocampus.

2623.1 mm²; Talairach coordinates: $x = -37.6$, $y = 15.5$, $z = 9.8$) extending to the pars triangularis, rostral middle frontal, caudal middle frontal and superior frontal cortices (Fig. 3A and Supplementary Fig. 1). As age increased, thickness decreased in the control group but not in family members (vertex-wise threshold of $P < 0.01$ corrected for multiple comparisons, Fig. 3B). There was no correlation between age and cortical thickness in the IFG [$r(4) = 0.40$, $P = 0.43$] after covarying for stuttering severity.

Bilateral middle frontal surface area is reduced in the family

A vertex-wise GLM corrected for multiple comparisons (controlling for age) revealed bilateral surface area reductions in the caudal middle frontal gyri in the family compared with controls. The right hemisphere cluster (cluster size: 1474.8 mm²; Talairach coordinates $x = 32.6$, $y = 18.7$, $z = 47.2$) extended into the inferior precentral gyrus. In the left hemisphere, the cluster (cluster size: 1196.3 mm²; Talairach coordinates: $x = -41.5$, $y = 3.5$, $z = 46.8$) extended from the caudal middle frontal into the middle precentral gyrus (Fig. 4). There was no correlation between age and surface area in the middle frontal gyri [right: $r(4) = -0.35$, $P = 0.50$; left: $r(4) = -0.03$, $P = 0.96$] after covarying for stuttering severity. There was no significant group by age interaction for surface area in any region. The GLM for local gyrification index revealed no differences

between the two groups in either hemisphere and no group by age interaction (all significance levels set at a vertex-wise threshold of $P < 0.01$, corrected for multiple comparisons).

The globus pallidus is larger bilaterally in affected family members

Bayesian Mann–Whitney analysis (Supplementary Table 1) indicated there was anecdotal evidence that differences in the volume of the pallidum could support the alternative hypothesis. Further analyses determined the family members had larger left ($U = 17$, $P = 0.017$; mean of increase 21%) and right ($U = 21$, $P = 0.037$, mean increase of 7%) globus pallidi. A larger right globus pallidus was associated with more severe stuttering ($\rho = 0.86$, $P = 0.01$; $BF_{10} = 4.2$).

No evidence of white matter differences between groups

When controlling for age, a multivariate ANCOVA revealed no group differences in tract volumes for the corticobulbar tract, CST, AF, or the FAT ($P > 0.15$). When analysed by hemisphere, neither fractional anisotropy nor mean diffusivity differed between family members and controls in any tract (all $P > 0.39$). Bayes factors suggested anecdotal evidence for increased fractional anisotropy in

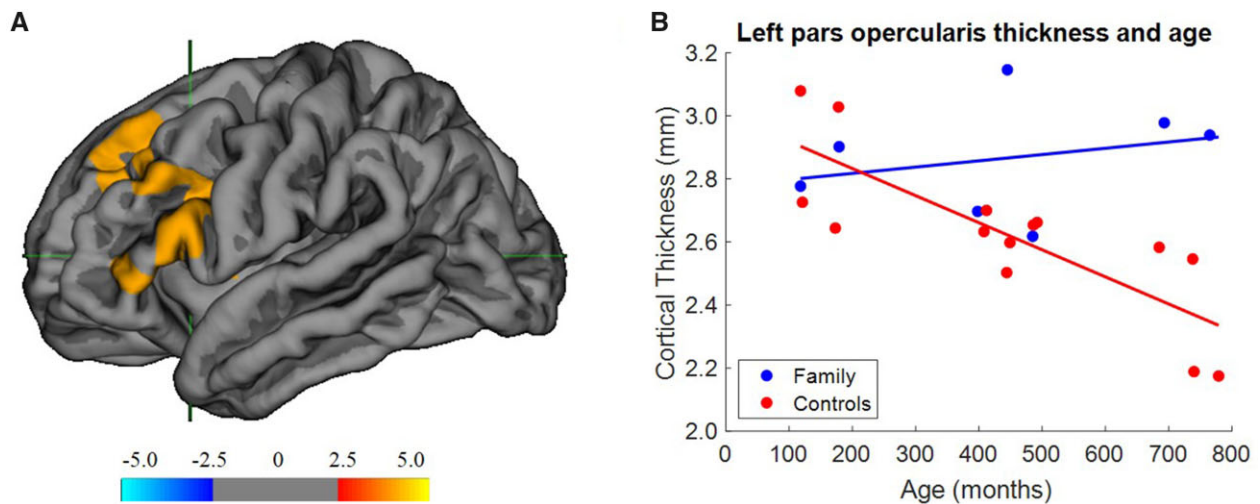


Figure 3 Atypical cortical thickness in Broca's area in the family. (A) Region where an age by group interaction is significant for cortical thickness. Peak cluster in the pars opercularis extends to the pars triangularis, rostral middle frontal, caudal middle frontal and superior frontal cortices. Colour bar indicates $-\log_{10}P$ value. (B) Cortical thickness of the pars opercularis in relation to age in the family ($n = 7$) and controls ($n = 14$).

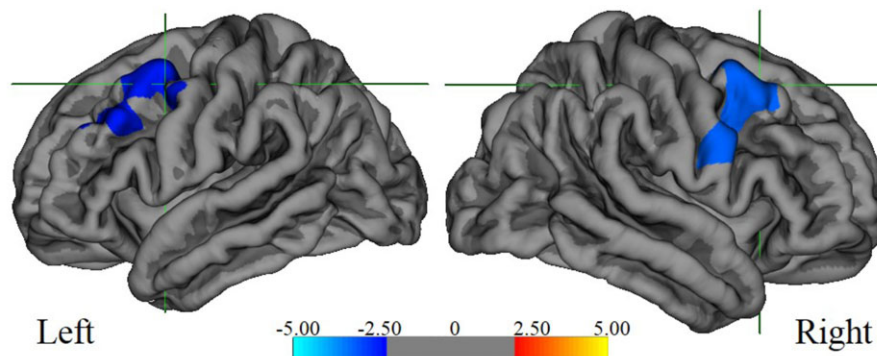


Figure 4 Surface area reductions in bilateral caudal middle gyri. Shaded blue regions indicate a decreased surface area in the family versus controls. Clusters are significant at $P < 0.01$ after Monte Carlo corrections. Colour bar indicates $-\log_{10}P$ value.

family members in the left CST and reduced mean diffusivity in left corticobulbar tract that could support the alternative hypothesis (Supplementary Table 2). All other Bayes factors were consistent that data were either more likely under the null hypothesis or provided insufficient evidence.

Genetic linkage mapping reveals loci on chromosomes 1 and 4

Inheritance of stuttering in this large four-generation family was consistent with an autosomal dominant pattern, with six instances of male-to-male transmission arguing against X-linkage, Y-linked or mitochondrial inheritance (Fig. 1). Males do not pass on their X-chromosome to male progeny, there are females in the family who stutter and who do not carry a Y chromosome, and males do not transmit mitochondrial DNA as it only comes from females via the oocyte, and not the sperm; for these reasons, the mode of transmission must be autosomal. We performed parametric linkage analysis in 16 family members (10 affected) assuming an autosomal dominant mode of inheritance with a rare dominant allele population frequency of 0.001, a penetrance of 0.0001 (phenocopy rate) for homozygous wild-type individuals and full penetrance (one) for heterozygous or homozygous carriers of the disease allele. Peak logarithm of odds scores of 3.0088 were found on chromosomes 1 and 4, as shown in Table 3 and Supplementary Table 3. Subsequent haplotype analysis at the loci on chromosomes 1 and 4 revealed that all 10 genotyped affected family members shared the same locus-specific haplotype at each locus indicating likely complete penetrance. Since the initial linkage analysis was performed with only a set of SNPs at an average spacing of 0.3 cm, we re-ran the analysis with the complete set of SNPs in the chromosome 1 and 4 regions to refine the haplotypes. This revealed that the originally identified locus on chromosome 1 was actually comprised of two adjacent loci as shown in Supplementary Table 4. A non-parametric linkage analysis performed using MERLIN failed to identify any additional regions (data not shown).

None of the three loci identified in the family overlap with eight known loci or genes for persistent developmental stuttering: GNPTAB (12q23.2; OMIM #607840), GNPTG (16p13.3; OMIM #607838), NAGPA (16p13.13; OMIM #607985), STUT1/AP4E1 (15q21.2; OMIM #184450/607244), STUT2 (12q24.1; OMIM #609261), STUT3 (3q13.2-q13.33; OMIM #614655) and STUT4 (16q12.1-q23.1; OMIM #614668) (Supplementary Table 4). Nor do they overlap with the eight known genes (CHD3, GLB1, GTS, NBIA1, PHARC, PRTS, SCYL1, SOX3) for syndromes associated with stuttering. The loci on chromosome 1 are 1a, comprising only two genes, and 1b, comprising over 200 genes. The locus on chromosome 4 comprises over 50 genes (Supplementary Table 4), indicating that there are many potential candidate genes. At the chromosome 1 loci, a number of genes have been associated with neurological disorders including childhood apraxia of speech (POGZ; OMIM #614787) as we recently described,⁶⁵ a neurodevelopmental disorder with brain malformations

(ARHGFE2; OMIM #607560) and severe developmental delay and intellectual disability (ASH1L OMIM #607999). Similarly, at the chromosome 4 locus, a number of genes have been associated with neurodevelopmental disorder with severe speech and language deficits (GRIA2; OMIM #138247), hyperekplexia (GLRB; OMIM #614619) and familial adult myoclonic epilepsy (RAPGEF2; OMIM #138492). However, none of these phenotypes overlap with persistent developmental stuttering.

Exome sequencing identifies several candidate genes expressed in critical brain regions

We performed exome sequencing on three affected family members and interrogated variation in the linkage regions on chromosomes 1 and 4 for novel or ultra-rare gene variants. We identified 28 variants (Supplementary Table 5) based on the criteria outlined in the 'Materials and methods' section, and a relevant known gene expression pattern or function (e.g. neuronal). None of these variants were in the genes outlined previously, and none of the genes in which they were located have an obvious phenotypic or functional link to stuttering. To ensure that other variants of interest were not missed, we performed Sanger sequencing of exons that had low depth of coverage on exome sequencing in the linked regions on chromosome 1 and 4. For this analysis, we prioritized 23 exons in 11 genes based on gene function and expression (e.g. neuronal genes expressed in brain), identifying eight new variants (Supplementary Table 6). None of the variants stood out as likely to be related to the phenotype, reflecting our lack of knowledge of genes causal for stuttering.

Discussion

We studied a large family with persistent developmental stuttering across four generations. Neuroimaging of seven affected family members revealed that Broca's area failed to follow the typical age-related thinning seen in the control group. Additionally, we found reduced surface area of the middle frontal gyri and enlarged bilateral globus pallidi. Taken together, these results point to an inherited disruption within the cortico-basal ganglia thalamo-cortical loop as a neural phenotype of stuttering.

By genotyping 16 affected or unaffected family members we identified novel loci on chromosomes 1 and 4 that map in an autosomal dominant mode with the stuttering phenotype. Notably, autosomal dominant inheritance of stuttering has already been reported, for example for the APE41 gene (STUT1 locus) in a large Cameroonian family.¹⁴ This demonstrates linkage mapping of single families does lead to reports of new loci. However, it should be noted that the fact that the inheritance in the Cameroonian family, and the family described in this report, appears to be autosomal dominant does not preclude the possibility that stuttering is a complex trait in other families or individuals with stuttering. Exome sequencing analysis has not revealed an obvious candidate gene segregating with stuttering in the family but did identify

Table 3 Linkage regions detected in family

Chromosome	Flankers and markers						LOD score
	Beginning of region			End of region			
	SNP	Physical position (bp)	Genetic position (cM)	SNP	Physical position (bp)	Genetic position (cM)	
1	rs655315	110 215 178	137.62	rs640692	175 739 003	191.62	3.0088
4	rs1869965	155 969 377	159.97	rs1021318	169 340 639	173.47	3.0088

several promising candidate genes expressed in critical brain regions. So far, we have not found variants in these genes in any of our other families or sporadic patients with stuttering.

Our cross-sectional data showed that cortical thickness remained relatively unchanged with age in Broca's area in affected family members. Lack of developmental thinning in the posterior part of Broca's area was also reported in a large cross-sectional study of unrelated children and adults with developmental stuttering,¹⁸ suggesting this is a consistent neural marker. There is strong evidence for functional anomalies in the pars opercularis in people who stutter, such as reduced cerebral blood flow at rest⁶⁶ and decreased oxygenated haemoglobin during speech tasks.⁴ In people with no history of stuttering, transcranial magnetic stimulation over Broca's area causes blocking during both overt and internal speech.⁶⁷ Our data indicate that genetically driven structural differences could underlie dysfunction in Broca's area and manifest as stuttering.

Interestingly, the younger members of the family demonstrated cortical thickness values within the range of their non-stuttering peers. We therefore suggest that cortical thickness per se is not directly related to stuttering, but rather evidence of a disrupted neurodevelopmental process. According to the expansion-renormalization model,⁶⁸ initial increases in cortical thickness due to practice or skill acquisition are followed by reduction and 'renormalization' within a few weeks. Cortical thinning is a genetically driven normal developmental process partly attributed to synaptic pruning and occurs latest in the frontal cortex.⁶⁹ The genetic variant linked to stuttering in this family may therefore inhibit or delay progression to the synaptic pruning process, resulting in the lack of typical developmental thinning in Broca's area.

Another critical finding in our study was an increase in size of the globus pallidus bilaterally in affected family members, and an association between stuttering severity and volume of the right globus pallidus. The role of the basal ganglia in the initiation and inhibition of movements is well documented⁷⁰ including in relation to fluent speech.⁷¹ Specifically, there is high connectivity between the globus pallidus (the main output structure of the basal ganglia with a primarily inhibitory function) and frontal cortex via the thalamus.⁷⁰ Adults can develop a stutter following disruption to the globus pallidus after deep brain stimulation⁷² and after lesions to the basal ganglia,⁷³ highlighting the importance of this network for fluency. The combination of an increase in globus pallidus size and Broca's area anomaly suggests a genetic origin of disrupted signalling between the two regions in affected family members. This disruption is in line with the hypothesis of an altered cortico-basal ganglia-thalamo-cortical loop in developmental stuttering.⁷⁴ In their review, Chang and Guenther⁷⁴ propose that this malfunctioning loop could result in stuttering by disrupting the timing, initiation/termination and sequencing of speech motor programs. They suggest malfunction could originate from multiple causes, namely structural basal ganglia anomalies, or connections at different levels within this loop.

The combination of an increase in globus pallidus size and Broca's area anomaly suggests a genetic origin of disrupted signalling between the two regions in affected family members. We propose that disrupted signalling from the globus pallidus to the thalamus affects the direct and indirect pathways of the cortico-basal ganglia-thalamo-cortical loop. This in turn results in both over activation of motor cortices (e.g. repeated syllables) and exacerbated inhibition of movement (e.g. blocking).

Our pars opercularis and globus pallidus findings are consistent with previous work⁷⁵ that reported positive psychophysiological interaction (PPI) between the two regions during an anticipatory task in unrelated adults who stutter, whereas controls showed a negative PPI. This study focused on the external segment of the

globus pallidus, however, Freesurfer does not yet have the capabilities to distinguish between the internal and external segments. Additionally, our structural findings do not inform functional connectivity. Nevertheless, our findings could be in agreement with the theory that a synchronicity between the globus pallidus and the IFG is related to increased activation of the indirect pathway, which would in turn increase the motor inhibition within the cortex in those who stutter.⁷⁵

More recently, limbic structures have also been examined in unrelated adults who stutter. An enlarged right nucleus accumbens led to the suggestion that this region may mediate between the limbic and motor systems during social speech.⁷⁶ Our *a priori* hypotheses regarding the basal ganglia did not account for the nucleus accumbens, however, an exploratory analysis *post hoc* (not reported) did not reveal any group difference. Including other previously overlooked subcortical areas in future MRI studies may increase our understanding of the neurobiology of developmental stuttering. For example, the habenula is known to play a pivotal role in negative reward⁷⁷ and, as with the nucleus accumbens, demonstrates disrupted connectivity to frontal motor areas after repeated dopaminergic exposure.⁷⁸ Further study on the role of the limbic-motor system in stuttered speech could have important treatment implications.

We further identified surface area reductions bilaterally in the posterior middle frontal gyri in the family. Given that the middle frontal gyrus sits at the interface between the ventral and dorsal attention networks,⁷⁹ we propose that the surface area reductions in affected family members indicate a deficiency in self-regulation and attention. These cognitive deficits have been commonly reported in both pre-schoolers⁸⁰ and adults who stutter.⁸¹

The macroanomalies identified within the family members were all deemed 'not clinically significant' by an experienced radiologist were in a range of locations, with few similarities between family members. No family member had previous MRI scans due to neurological symptoms or concerns. Although we cannot completely rule out that anomalies may have affected downstream cortical measurements within the Freesurfer pipeline, we thoroughly checked registration to the template and observed no issues. Additional analyses excluding either regions or participants of concern replicated initial results, thus demonstrating the robustness of our findings. It is difficult to argue a causal link between the stuttering phenotype and these cortical variations given their inconsistent locations. We currently hypothesize they are a by-product of a genetic variant that, unexpectedly, alters brain development in a heterogenous manner.

Based on our Bayesian analyses, selected as a more viable alternative to frequentist analyses due to its capabilities to account for small sample size, we found no evidence for reduced fractional anisotropy in the family in the arcuate or FATs. Notwithstanding, we should not discount the alternative interpretation of our results; that our sample may not have been sufficient to detect group differences. However, from our findings, overall, we have little evidence that white matter disruptions are the main consequence of genetic aberration, and instead propose that grey matter anomalies are more likely causal links to stuttering within this family.

In summary, in this family with autosomal dominant persistent stuttering, we have identified two novel chromosomal loci without finding the underlying pathogenic variant. Our neuroimaging findings suggest an imbalance of cortical inhibition within the cortico-basal ganglia-thalamo-cortical speech network. This disruption is associated with structural differences in Broca's area and the globus pallidus with large effect sizes. Normalization of this network using a behavioural or pharmacological intervention could provide an avenue for personalized treatment.

Acknowledgements

The authors thank the family for their participation. We thank Dr Terry Lorenz for his input on Bayesian statistical analyses. We thank Simone Mendelstam (S.M.) for her radiological reports.

Funding

This study was supported by the National Health and Medical Research Council Centre of Research Excellence (1116976) and a Project Grant (1127144) to A.T.M., M.S.H., F.J.L., A.C., I.E.S. and M.B.; Practitioner Fellowships to A.T.M. (1105008), I.E.S. (1006110); a Senior Research Fellowship to M.B. (1102971), a R.D Wright Career Development Fellowship (1063799) to M.S.H. and a Postgraduate Scholarship to S.J.T. (1017773). A.T.M., S.B. and M.B. were supported by the Victorian Government's Operational Infrastructure Support Program and Australian Government National Health and Medical Research Council Independent Research Institute Infrastructure Support Scheme (NHMRC IRIISS). All research at Great Ormond Street Hospital NHS Foundation Trust and UCL Great Ormond Street Institute of Child Health (F.L. and D.T.-L.) is made possible by the NIHR Great Ormond Street Hospital Biomedical Research Centre. The views expressed are those of the authors and not necessarily those of the NHS, the NIHR or the Department of Health. I.H. was supported by The Hartwell Foundation through an Individual Biomedical Research Award and by the National Institute for Neurological Disorders and Stroke (K02 NS112600).

Competing interests

The authors report no competing interests.

Supplementary material

Supplementary material is available at *Brain* online.

References

1. Yairi E, Ambrose N. Epidemiology of stuttering: 21st century advances. *J Fluency Disord.* 2013;38(2):66–87.
2. Kefalianos E, Onslow M, Packman A, et al. The history of stuttering by 7 years of age: Follow-up of a prospective community cohort. *J Speech Lang Hear Res.* 2017;60(10):2828–2839.
3. Craig A, Hancock K, Tran Y, Craig M, Peters K. Epidemiology of stuttering in the community across the entire life span. *J Speech Lang Hear Res.* 2002;45(6):1097–1105.
4. Walsh B, Tian F, Tourville JA, et al. Hemodynamics of speech production: An fNIRS investigation of children who stutter. *Sci Rep.* 2017;7(1):4034.
5. Gerlach H, Totty E, Subramanian A, Zebrowski P. Stuttering and labor market outcomes in the United States. *J Speech Lang Hear Res.* 2018;61(7):1649–1663.
6. Klompas M, Ross E. Life experiences of people who stutter, and the perceived impact of stuttering on quality of life: Personal accounts of South African individuals. *J Fluency Disord.* 2004;29(4):275–305.
7. Nang C, Hersh D, Milton K, Lau SR. The impact of stuttering on development of self-identity, relationships, and quality of life in women who stutter. *Am J Speech Lang Pathol.* 2018;27(3S):1244–1258.
8. Gunn A, Menzies RG, O'Brian S, et al. Axis I anxiety and mental health disorders among stuttering adolescents. *J Fluency Disord.* 2014;40:58–68.
9. Frigerio-Domingues C, Drayna D. Genetic contributions to stuttering: The current evidence. *Mol Genet Genomic Med.* 2017;5(2):95–102.
10. Kang C, Drayna D. Genetics of speech and language disorders. *Annu Rev Genomics Hum Genet.* 2011;12:145–164.
11. Kang C, Riazuddin S, Mundorff J, et al. Mutations in the lysosomal enzyme-targeting pathway and persistent stuttering. *N Engl J Med.* 2010;362(8):677–685.
12. Chow HM, Garnett EO, Li H, et al. Linking lysosomal enzyme targeting genes and energy metabolism with altered gray matter volume in children with persistent stuttering. *Neurobiol Lang.* 2020;1(3):365–380.
13. Benito-Aragón C, Gonzalez-Sarmiento R, Liddell T, et al. Neurofilament-lysosomal genetic intersections in the cortical network of stuttering. *Prog Neurobiol.* 2020;184:101718.
14. Raza MH, Mattera R, Morell R, et al. Association between rare variants in AP4E1, a component of intracellular trafficking, and persistent stuttering. *Am J Hum Genet.* 2015;97(5):715–725.
15. Watkins KE, Vargha-Khadem F, Ashburner J, et al. MRI analysis of an inherited speech and language disorder: Structural brain abnormalities. *Brain.* 2002;125(Pt 3):465–478.
16. Liegeois F, J, et al. Early neuroimaging markers of FOXP2 intragenic deletion. *Sci Rep.* 2016;6:35192.
17. Liegeois FJ, et al. Dorsal language stream anomalies in an inherited speech disorder. *Brain.* 2019;142:966–977.
18. Beal DS, Lerch JP, Cameron B, et al. The trajectory of gray matter development in Broca's area is abnormal in people who stutter. *Front Hum Neurosci.* 2015;9:89.
19. Chang SE, Zhu DC, Choo AL, Angstadt M. White matter neuro-anatomical differences in young children who stutter. *Brain.* 2015;138(Pt 3):694–711.
20. Garnett EO, Chow HM, Nieto-Castañón A, et al. Anomalous morphology in left hemisphere motor and premotor cortex of children who stutter. *Brain.* 2018;141(9):2670–2684.
21. Lu C, Chen C, Peng D, et al. Neural anomaly and reorganization in speakers who stutter: A short-term intervention study. *Neurology.* 2012;79(7):625–632.
22. Etchell AC, Civier O, Ballard KJ, Sowman PF. A systematic literature review of neuroimaging research on developmental stuttering between 1995 and 2016. *J Fluency Disord.* 2018;55:6–45.
23. Cai S, Tourville JA, Beal DS, et al. Diffusion imaging of cerebral white matter in persons who stutter: Evidence for network-level anomalies. *Front Hum Neurosci.* 2014;8:54.
24. Chang SE. Using brain imaging to unravel the mysteries of stuttering. *Cerebrum.* 2011;2011:12.
25. Chang SE, Zhu DC. Neural network connectivity differences in children who stutter. *Brain.* 2013;136(Pt 12):3709–3726.
26. Cieslak M, Ingham RJ, Ingham JC, Grafton ST. Anomalous white matter morphology in adults who stutter. *J Speech Lang Hear Res.* 2015;58(2):268–277.
27. Connally EL, Ward D, Howell P, Watkins KE. Disrupted white matter in language and motor tracts in developmental stuttering. *Brain Lang.* 2014;131:25–35.
28. Kronfeld-Duenias V, Amir O, Ezrati-Vinacour R, Civier O, Ben-Shachar M. Dorsal and ventral language pathways in persistent developmental stuttering. *Cortex.* 2016;81:79–92.
29. Hickok G. Computational neuroanatomy of speech production. *Nat Rev Neurosci.* 2012;13(2):135–145.
30. Catani M, Dell'acqua F, Vergani F, et al. Short frontal lobe connections of the human brain. *Cortex.* 2012;48(2):273–291.
31. Dick AS, Garic D, Graziano P, Tremblay P. The frontal aslant tract (FAT) and its role in speech, language and executive function. *Cortex.* 2019;111:148–163.

32. Kronfeld-Duenias V, Amir O, Ezrati-Vinacour R, Civier O, Ben-Shachar M. The frontal aslant tract underlies speech fluency in persistent developmental stuttering. *Brain Struct Funct.* 2016; 221(1):365–381.
33. Misaghi E, Zhang Z, Gracco VL, De Nil LF, Beal DS. White matter tractography of the neural network for speech-motor control in children who stutter. *Neurosci Lett.* 2018;668:37–42.
34. Lu C, Peng D, Chen C, et al. Altered effective connectivity and anomalous anatomy in the basal ganglia-thalamocortical circuit of stuttering speakers. *Cortex.* 2010;46(1):49–67.
35. Jancke L, Hanggi J, Steinmetz H. Morphological brain differences between adult stutterers and non-stutterers. *BMC Neurol.* 2004; 4(1):23.
36. Kell CA, Neumann K, von Kriegstein K, et al. How the brain repairs stuttering. *Brain.* 2009;132(Pt 10):2747–2760.
37. Beal DS, Gracco VL, Brettschneider J, Kroll RM, De Nil LF. A voxel-based morphometry (VBM) analysis of regional grey and white matter volume abnormalities within the speech production network of children who stutter. *Cortex.* 2013;49(8): 2151–2161.
38. Cai S, Beal DS, Ghosh SS, Guenther FH, Perkell JS. Impaired timing adjustments in response to time-varying auditory perturbation during connected speech production in persons who stutter. *Brain Lang.* 2014;129:24–29.
39. Chang SE, Erickson KI, Ambrose NG, Hasegawa-Johnson MA, Ludlow CL. Brain anatomy differences in childhood stuttering. *NeuroImage.* 2008;39(3):1333–1344.
40. Beal DS, Gracco VL, Lafaille SJ, De Nil LF. Voxel-based morphometry of auditory and speech-related cortex in stutterers. *Neuroreport.* 2007;18(12):1257–1260.
41. Song LP, et al. Gray matter abnormalities in developmental stuttering determined with voxel-based morphometry. *Zhonghua Yi Xue Za Zhi.* 2007;87:2884–2888.
42. Sowman PF, Ryan M, Johnson BW, et al. Grey matter volume differences in the left caudate nucleus of people who stutter. *Brain Lang.* 2017;164:9–15.
43. Foundas AL, Mock JR, Cindass R Jr, Corey DM. Atypical caudate anatomy in children who stutter. *Percept Mot Skills.* 2013;116(2): 528–543.
44. Wechsler D. *Wechsler abbreviated scale of intelligence, 2nd edn (WASI-II)*. Pearson; 2011.
45. Bahlo M, Bromhead CJ. Generating linkage mapping files from Affymetrix SNP chip data. *Bioinformatics.* 2009;25(15):1961–1962.
46. Abecasis GR, Cherny SS, Cookson WO, Cardon LR. Merlin-rapid analysis of dense genetic maps using sparse gene flow trees. *Nat Genet.* 2002;30(1):97–101.
47. Thiele H, Nurnberg P. HaploPainter: A tool for drawing pedigrees with complex haplotypes. *Bioinformatics.* 2005;21(8):1730–1732.
48. Dale AM, Fischl B, Sereno MI. Cortical surface-based analysis. I. Segmentation and surface reconstruction. *NeuroImage.* 1999; 9(2):179–194.
49. Fischl B, Dale AM. Measuring the thickness of the human cerebral cortex from magnetic resonance images. *Proc Natl Acad Sci USA.* 2000;97(20):11050–11055.
50. Fischl B, Sereno MI, Dale AM. Cortical surface-based analysis. II: Inflation, flattening, and a surface-based coordinate system. *NeuroImage.* 1999;9(2):195–207.
51. Tournier J-D, Smith R, Raffelt D, et al. MRtrix3: A fast, flexible and open software framework for medical image processing and visualisation. *NeuroImage.* 2019;202:116137.
52. Veraart J, Novikov DS, Christiaens D, et al. Denoising of diffusion MRI using random matrix theory. *NeuroImage.* 2016;142:394–406.
53. Andersson JL, Skare S, Ashburner J. How to correct susceptibility distortions in spin-echo echo-planar images: Application to diffusion tensor imaging. *NeuroImage.* 2003;20(2):870–888.
54. Andersson JLR, Sotiropoulos SN. An integrated approach to correction for off-resonance effects and subject movement in diffusion MR imaging. *NeuroImage.* 2016;125:1063–1078.
55. Smith SM, Jenkinson M, Woolrich MW, et al. Advances in functional and structural MR image analysis and implementation as FSL. *NeuroImage.* 2004;23 (Suppl 1):S208–219.
56. Tustison NJ, Avants BB, Cook PA, et al. N4ITK: Improved N3 bias correction. *IEEE Trans Med Imaging.* 2010;29(6):1310–1320.
57. Tournier JD, Calamante F, Connelly A. Robust determination of the fibre orientation distribution in diffusion MRI: Non-negativity constrained super-resolved spherical deconvolution. *NeuroImage.* 2007;35(4):1459–1472.
58. Liégeois FJ, Mahony K, Connelly A, et al. Pediatric traumatic brain injury: Language outcomes and their relationship to the arcuate fasciculus. *Brain Lang.* 2013;127(3):388–398.
59. Ourselin S, Roche A, Subsol G, Pennec X, Ayache N. Reconstructing a 3D structure from serial histological sections. *Image Vis Comput.* 2001;19(1-2):25–31.
60. Modat M, Cash DM, Daga P, et al. Global image registration using a symmetric block-matching approach. *J Med Imaging (Bellingham, Wash.).* 2014;1(2):024003.
61. Rueckert D, Sonoda LI, Hayes C, et al. Nonrigid registration using free-form deformations: Application to breast MR images. *IEEE Trans Med Imaging.* 1999;18(8):712–721.
62. Modat M, Ridgway GR, Taylor ZA, et al. Fast free-form deformation using graphics processing units. *Comput Methods Programs Biomed.* 2010;98(3):278–284.
63. Tzourio-Mazoyer N, Landeau B, Papathanassiou D, et al. Automated anatomical labeling of activations in SPM using a macroscopic anatomical parcellation of the MNI MRI single-subject brain. *NeuroImage.* 2002;15(1):273–289.
64. JASP Team. JASP (version 0.14.1); 2020.
65. Hildebrand MS, Jackson VE, Scerri TS, et al. Severe childhood speech disorder: Gene discovery highlights transcriptional dysregulation. *Neurology.* 2020;94(20):e2148–e2167.
66. Desai J, Huo Y, Wang Z, et al. Reduced perfusion in Broca’s area in developmental stuttering. *Hum Brain Mapp.* 2017;38(4): 1865–1874.
67. Aziz-Zadeh L, Cattaneo L, Rochat M, Rizzolatti G. Covert speech arrest induced by rTMS over both motor and nonmotor left hemisphere frontal sites. *J Cogn Neurosci.* 2005;17(6):928–938.
68. Wenger E, Brozzoli C, Lindenberger U, Lövdén M. Expansion and renormalization of human brain structure during skill acquisition. *Trends Cogn Sci.* 2017;21(12):930–939.
69. Fjell AM, Grydeland H, Krogstad SK, et al. Development and aging of cortical thickness correspond to genetic organization patterns. *Proc Natl Acad Sci USA.* 2015;112(50):15462–15467.
70. Yin HH, Knowlton BJ. The role of the basal ganglia in habit formation. *Nat Rev Neurosci.* 2006;7(6):464–476.
71. Chang SE, Garnett EO, Etchell A, Chow HM. Functional and neuroanatomical bases of developmental stuttering: Current insights. *Neuroscientist.* 2019;25(6):566–582.
72. Nebel A, Reese R, Deuschl G, Mehdorn HM, Volkman J. Acquired stuttering after pallidal deep brain stimulation for dystonia. *J Neural Transm (Vienna).* 2009;116(2):167–169.
73. Lundgren K, Helm-Estabrooks N, Klein R. Stuttering following acquired brain damage: A review of the literature. *J Neurolinguistics.* 2010;23(5):447–454.
74. Chang S-E, Guenther FH. Involvement of the cortico-basal ganglia-thalamocortical loop in developmental stuttering. *Front Psychol.* 2019;10:3088–3088.
75. Metzger FL, Auer T, Helms G, et al. Shifted dynamic interactions between subcortical nuclei and inferior frontal gyri during response preparation in persistent developmental stuttering. *Brain Struct Funct.* 2018;223(1):165–182.

76. Neef NE, Bütfering C, Auer T, et al. Altered morphology of the nucleus accumbens in persistent developmental stuttering. *J Fluency Disord.* 2018;55:84–93.
77. Salas R, Baldwin P, de Biasi M, Montague PR. BOLD responses to negative reward prediction errors in human habenula. *Front Hum Neurosci.* 2010;4:36.
78. Savjani RR, Velasquez KM, Thompson-Lake DGY, et al. Characterizing white matter changes in cigarette smokers via diffusion tensor imaging. *Drug Alcohol Depend.* 2014;145:134–142.
79. Corbetta M, Patel G, Shulman GL. The reorienting system of the human brain: From environment to theory of mind. *Neuron.* 2008;58(3):306–324.
80. Karrass J, Walden TA, Conture EG, et al. Relation of emotional reactivity and regulation to childhood stuttering. *J Commun Disord.* 2006;39(6):402–423.
81. Eichorn N, Pirutinsky S, Marton K. Effects of different attention tasks on concurrent speech in adults who stutter and fluent controls. *J Fluency Disord.* 2019;61:105714.